



Linearmycins Activate a Two-Component Signaling System Involved in Bacterial Competition and Biofilm Morphology

Reed M. Stubbendieck^{a,b}  Paul D. Straight^{a,b} 

Interdisciplinary Program in Genetics, Texas A&M University, College Station, Texas, USA^a; Department of Biochemistry & Biophysics, Texas A&M University, College Station, Texas, USA^b

ABSTRACT Bacteria use two-component signaling systems to adapt and respond to their competitors and changing environments. For instance, competitor bacteria may produce antibiotics and other bioactive metabolites and sequester nutrients. To survive, some species of bacteria escape competition through antibiotic production, biofilm formation, or motility. Specialized metabolite production and biofilm formation are relatively well understood for bacterial species in isolation. How bacteria control these functions when competitors are present is not well studied. To address fundamental questions relating to the competitive mechanisms of different species, we have developed a model system using two species of soil bacteria, *Bacillus subtilis* and *Streptomyces* sp. strain Mg1. Using this model, we previously found that linearmycins produced by *Streptomyces* sp. strain Mg1 cause lysis of *B. subtilis* cells and degradation of colony matrix. We identified strains of *B. subtilis* with mutations in the two-component signaling system *yfiJK* operon that confer dual phenotypes of specific linearmycin resistance and biofilm morphology. We determined that expression of the ATP-binding cassette (ABC) transporter *yfiLMN* operon, particularly *yfiM* and *yfiN*, is necessary for biofilm morphology. Using transposon mutagenesis, we identified genes that are required for YfiLMN-mediated biofilm morphology, including several chaperones. Using transcriptional fusions, we found that YfiJ signaling is activated by linearmycins and other polyene metabolites. Finally, using a truncated YfiJ, we show that YfiJ requires its transmembrane domain to activate downstream signaling. Taken together, these results suggest coordinated dual antibiotic resistance and biofilm morphology by a single multifunctional ABC transporter promotes competitive fitness of *B. subtilis*.

IMPORTANCE DNA sequencing approaches have revealed hitherto unexplored diversity of bacterial species in a wide variety of environments that includes the gastrointestinal tract of animals and the rhizosphere of plants. Interactions between different species in bacterial communities have impacts on our health and industry. However, many approaches currently used to study whole bacterial communities do not resolve mechanistic details of interspecies interactions, including how bacteria sense and respond to their competitors. Using a competition model, we have uncovered dual functions for a previously uncharacterized two-component signaling system involved in specific antibiotic resistance and biofilm morphology. Insights gleaned from signaling within interspecies interaction models build a more complete understanding of gene functions important for bacterial communities and will enhance community-level analytical approaches.

KEYWORDS ABC transporter, antibiotics, antibiotic resistance, *Bacillus subtilis*, biofilm, linearmycin, polyene, *Streptomyces*, two-component signaling

Bacteria within communities require signaling mechanisms to respond to changing environments and challenges from other species. Although neighboring cells may cooperate, competition is likely to be the dominant mode of interaction between

Received 15 March 2017 **Accepted** 24 April 2017

Accepted manuscript posted online 1 May 2017

Citation Stubbendieck RM, Straight PD. 2017. Linearmycins activate a two-component signaling system involved in bacterial competition and biofilm morphology. *J Bacteriol* 199:e00186-17. <https://doi.org/10.1128/JB.00186-17>.

Editor Ann M. Stock, Rutgers University-Robert Wood Johnson Medical School

Copyright © 2017 American Society for Microbiology. All Rights Reserved.

Address correspondence to Paul D. Straight, paul_straight@tamu.edu.

bacteria in nature (1). Bacteria have evolved numerous mechanisms to compete with their neighbors. These competitive mechanisms include production of specialized metabolites, including antibiotics, contact-dependent inhibition systems, and type VI secretion systems that directly deliver toxins into cells, among others (reviewed in reference 2). Individual cells or aggregates of cells either adapt to competition or suffer fitness costs (3). Therefore, to avoid loss of fitness and survive, bacteria integrate and respond to external signals that indicate changing environments and threats from competitor species.

One of the primary mechanisms that bacteria use to monitor their environment is two-component signaling (TCS). TCS systems are often used to sense abiotic signals such as levels of oxygen and other nutrients. Bacteria also sense and respond to biotic signals that indicate the presence of competitors. Examples of biotic signals include changes in available external nutrients (4), the presence of antibiotics (5–8), and direct monitoring of the cell envelope (9). The *Bacillus subtilis* genome contains genes for 30 complete TCS system pairs (10). Functions for many of the *B. subtilis* TCS systems have been defined and include maintenance of metabolic homeostasis, nutrient uptake, and cell envelope structure. However, numerous TCS system functions remain unknown, principally because their corresponding loss-of-function mutants have no phenotype under standard laboratory conditions. While many of these TCS systems are nonessential under laboratory conditions, their presence in the genome suggests they provide selective advantages in competitive environments.

The cell envelope, which functions as the interface of bacterial cells and their environment, is a common target for antibiotics. Excessive damage to this essential structure is lethal (11–13). Therefore, bacterial cells have mechanisms to monitor the condition of their envelopes in response to damage (14, 15). Accordingly, of the 30 complete TCS system pairs carried by the *B. subtilis* genome (10), currently 10 are known to be involved in the regulation and maintenance of the cell envelope and resistance to antibiotics that target these structures (15–27). The signal receptors may monitor direct damage to the wall or indirect disruptions to metabolism that perturb membrane physiology. For example, it has been demonstrated that the histidine kinase PhoR senses intermediates of wall teichoic acid synthesis as a proxy for cellular phosphate levels (26), and the histidine kinase KinC senses potassium ion (K⁺) leakage (28). Identifying the targets and signals that activate unknown TCS systems may reveal new therapeutic targets for targeted drug design and circumvention of adaptive cellular responses.

This study focuses on a TCS-mediated response to linearmycins, a family of antibiotic-specialized metabolites produced by some streptomycetes (29, 30). The linearmycins induce progressive lysis and degradation of *B. subtilis* cultured next to *Streptomyces* sp. strain Mg1 (27, 31). We previously identified point mutations in the *yfiJK* operon, encoding a TCS system responsible for *B. subtilis* linearmycin resistance (27). Deletion of the *yfiJK* operon had no effect on lysis when *B. subtilis* was cultured with *Streptomyces* sp. strain Mg1, suggesting that resistance arises from activation of the TCS. Indeed, we found that strains of *B. subtilis* with the *yfiJK* point mutations increased expression of the *yfiLMN* operon, encoding an ATP-binding cassette (ABC) transporter necessary for linearmycin resistance. In addition to resistance, we observed that the mutants form biofilm-like colonies on rich media, suggesting that the YfiJK system promotes biofilm formation.

In the present study, we investigated how *B. subtilis* linearmycin-resistant mutations cause colonies to have biofilm morphology. We find that YfiK exclusively regulates the expression of the *yfiLMN* operon. We show that biofilm morphology is dependent upon the YfiLMN ABC transporter. Notably, the cytoplasmic ATPase encoded by *yfiL* is dispensable for biofilm morphology, indicating that a functional ABC transporter is needed only for linearmycin resistance. Using transposon mutagenesis, we identified additional genes that, while not differentially regulated in linearmycin-resistant mutants, are nonetheless required for biofilm morphology. To monitor YfiJK activity, we used a transcriptional fusion of the *yfiLMN* promoter to *lacZ* as a reporter. We show that the YfiJK TCS induces expression of the *yfiLMN* operon in response to linearmycins and

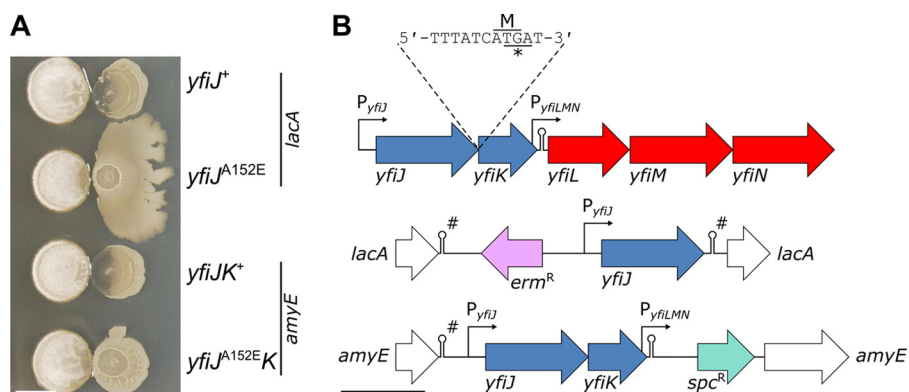


FIG 1 Genetic complementation of *yfiJ* confers linearmycin resistance and colony morphology phenotypes. (A) Wild-type *Streptomyces* sp. strain Mg1 (PDS0543) colonies (left) were cocultured with *B. subtilis* colonies (right). The strains of *B. subtilis* with *yfiJ*⁺ (PDS0571) and *yfiJ*^{A152E} (PDS0572) were complemented at the *lacA* locus as monocistrons with the native promoter and a plasmid-derived terminator. The strains of *B. subtilis* with *yfiJK*⁺ (PDS0627) and *yfiJ*^{A152E}*K* (PDS0685) were complemented at the *amyE* locus with their native operon structure, including the promoter and terminator. Strains with *yfiJ*^{A152E} alleles are resistant to linearmycin-induced lysis, which is observed adjacent to *Streptomyces* sp. strain Mg1 for strains with wild-type alleles. Colony spreading occurs with the *yfiJ*^{A152E} strain but is absent from the *yfiJ*^{A152E}*K* strain. The photograph was taken after 72 h of cocultivation on MYM agar. The photograph is representative of triplicate samples. The scale bar is 5 mm. (B, top) The configuration for *yfiJK-LMN* at the native chromosome locus. The overlapping stop codon in *yfiJ* and start codon in *yfiK* are marked with an asterisk and the letter M, respectively. (Middle) The monocistronic complementation construct for *yfiJ* inserted at *lacA*. (Bottom) The bicistronic complementation construct for *yfiJK* inserted at *amyE*. Open reading frames are shown as block arrows, promoters are shown as arrows, and intrinsic terminators are shown as hairpins. #, plasmid-derived terminators. The scale bar is 1 kb. *erm*^R, erythromycin resistance cassette; *spc*^R, spectinomycin resistance cassette.

other polyenes. Together, the data demonstrate how *B. subtilis* responds to linearmycin stress imposed by *Streptomyces* sp. strain Mg1, specifically regulating production of the YfiLMN multifunctional ABC transporter, resulting in both biofilm morphology and linearmycin resistance functions. The results provide new insight into the function of TCS systems and ABC transporters in *B. subtilis*, suggesting that concerted activation of specific linearmycin resistance and biofilm formation promotes *B. subtilis* fitness when faced with competitive challenge by *Streptomyces* sp. strain Mg1.

RESULTS

***yfiJK* configuration influences colony phenotypes.** Gain-of-function point mutations within the *yfiJK* operon cause *B. subtilis* to become resistant to linearmycins (Fig. 1A) (27). We identified nine mutations within the histidine kinase-encoding gene *yfiJ* and a single mutation in *yfiK*, which encodes the cognate response regulator. Both open reading frames (ORFs) are part of a single transcript, as the *yfiJ* stop and *yfiK* start codons overlap, and *yfiK* lacks its own promoter (Fig. 1B). Global expression profiles of *B. subtilis* confirm that *yfiJ* and *yfiK* are part of a bicistronic mRNA (32). When complementing their respective deletion strains, all identified point mutations resulted in linearmycin resistance (27).

We noticed phenotypic variation for the *yfiJ*^{A152E} allele depending on the complementation configuration. Previously, we complemented the *yfiJ* deletion strain with monocistronic *yfiJ*^{A152E}. Reproducibly, the colony of this *B. subtilis* strain spread across the agar surface when cultured next to *Streptomyces* sp. strain Mg1 (Fig. 1A). However, when complemented with the bicistronic *yfiJ*^{A152E}*K*, the *B. subtilis* colony did not spread in response to *Streptomyces* sp. strain Mg1 but was linearmycin resistant and developed biofilm morphology (Fig. 1A). Otherwise, we have observed no phenotypic differences between these strains, including monoculture growth rate. We hypothesized the phenotypic variation results from differences in gene expression arising from the complementing fragments. For example, the expression levels from the complementation loci (*amyE* versus *lacA*), the relative strength of the native (−9.30 kcal/mol) and plasmid-derived (−13.20 kcal/mol) intrinsic terminators we used, or simply disruption

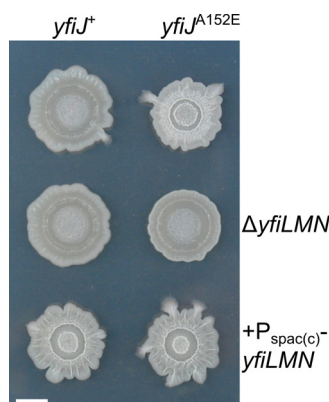


FIG 2 Biofilm morphology of linearmycin-resistant mutants is dependent upon *yfiLMN*. The *yfiJ*⁺ strain (PDS0571) develops as a smooth colony, but the *yfiJ*^{A152E} colony (PDS0572) has biofilm morphology. Deletion of *yfiLMN* reverts the biofilm morphology of the *yfiJ*^{A152E} colony (PDS0799) back to smooth. Complementation of the *yfiLMN* deletion with constitutively expressed *yfiLMN* [*P*_{spac(c)}-*yfiLMN*] causes both *yfiJ*⁺ (PDS0801) and *yfiJ*^{A152E} (PDS0802) colonies to have biofilm morphologies. The photograph was taken after 48 h of incubation on MYM agar and is representative of duplicate samples. The scale bar is 5 mm.

of regulatory functions dependent on the bicistronic arrangement of *yfiJK* could explain the differences between the *yfiJ*^{A152E} monocistronic and *yfiJ*^{A152EK} bicistronic complements.

The YfiJK system regulates a single operon. We wanted to determine if the variation observed reflects different levels of YfiJK activation from the *yfiJ*^{A152E} and *yfiJ*^{A152EK} complementing strains. Previously, we used RNA sequencing to compare the transcriptomes of the engineered *yfiJ*^{A152EK} and the *yfiJK*⁺ strains. The only significantly upregulated ORFs were in the downstream *yfiLMN* operon (see Fig. S1A in the supplemental material) (27). We also identified *des* and the *yvfRS* operon as moderately downregulated by YfiK. However, using quantitative reverse transcription-PCR (qRT-PCR), we have found no reproducible pattern of change in either *des* or *yvfS* expression (Fig. S2). Also, artificial overexpression of *des* from a xylose-inducible promoter had no impact on linearmycin resistance or colony morphology (Fig. S3). Taken together, these results suggest that the *yfiLMN* operon is the only target directly regulated by YfiK.

To compare strains expressing different alleles of *yfiJ*, we focused on expression of the downstream *yfiLMN* operon. We identified a single active promoter within 150 bp upstream of *yfiL* and no promoter sequences within *yfiL*, *yfiM*, or *yfiN* (Fig. 1B). Therefore, we used qRT-PCR to compare the relative fold expression of *yfiL* between engineered strains either with $\Delta yfiJ$ *yfiJ*^{A152E} only or with $\Delta yfiJK$ *yfiJ*^{A152EK}. In the $\Delta yfiJ$ *yfiJ*^{A152E} strain, we found that the expression of *yfiL* was ~135-fold higher than that of $\Delta yfiJ$ *yfiJ*⁺ (Fig. S2). In comparison, the expression of *yfiL* in the $\Delta yfiJK$ *yfiJ*^{A152EK} strain was ~20-fold higher than that of the $\Delta yfiJK$ *yfiJK*⁺ strain (27). The different transcript abundances indicate that the increased colony-spreading exhibited by the $\Delta yfiJ$ *yfiJ*^{A152E} strain is due to the higher level of increased expression of the *yfiLMN* operon. Given the enhanced morphology and colony-spreading phenotypes, we chose to use the $\Delta yfiJ$ *yfiJ*^{A152E} strain for subsequent experiments.

Elevated expression of the *yfiLMN* operon causes *B. subtilis* colonies to develop biofilm morphology. In monoculture, strains with the *yfiJ*^{A152E} allele develop colonies with a rough texture and a characteristic circular wrinkle in the center of the colony (Fig. 2). For simplicity and because the morphology is dependent upon extracellular polysaccharides (EPS), we will refer to these colonies as having biofilm morphology (27). In contrast, strains with a wild-type *yfiJ*⁺ allele develop relatively flat and featureless colonies (Fig. 2). Because the *yfiLMN* operon is the target of YfiJK regulation, we suspected that production of the YfiLMN ABC transporter would be responsible for

TABLE 1 YfiLMN functions in linearmycin and biofilm morphology

Strain description ^a	Finding for ^b :			
	Linearmycin resistance		Biofilm morphology	
	yfiJ ⁺	yfiJ ^{A152E}	yfiJ ⁺	yfiJ ^{A152E}
yfiLMN ⁺	–	+	–	+
ΔyfiLMN	–	–	–	–
ΔyfiLMN P _{spac(c)} -yfiLMN	+	+	+	+
ΔyfiL	–	–	–	+
ΔyfiM	–	–	–	–
ΔyfiN	–	–	–	–

^aWild-type alleles are designated with a superscript plus symbol. The P_{spac(c)}-yfiLMN strains constitutively express yfiLMN regardless of yfiJ allele.

^bThe plus and minus symbols indicate the presence or absence, respectively, of linearmycin resistance in coculture with *Streptomyces* sp. strain Mg1 or biofilm morphology in monoculture on MYM.

promoting biofilm morphology. To test this hypothesis, we constructed a deletion of the yfiLMN operon in both the yfiJ⁺ and yfiJ^{A152E} strain backgrounds. In addition to rendering *B. subtilis* sensitive to linearmycin, the yfiJ^{A152E} ΔyfiLMN strain forms a colony that is indistinguishable from the wild type (Fig. 2 and Table 1). When we complemented the yfiLMN deletion with a constitutively expressed copy of the yfiLMN operon [P_{spac(c)}-yfiLMN], both resistance and biofilm morphology were restored, regardless of yfiJ allele (Fig. 2).

We asked if a functional ABC transporter is necessary for both linearmycin resistance and biofilm formation. ABC transporters typically are comprised of two copies of a cytoplasmic nucleotide-binding domain (NBD) protein, which provides energy through ATP hydrolysis, and two membrane-spanning domains (MSDs) that form the pore (33). In the case of YfiLMN, the NBD is encoded by yfiL and the MSDs are encoded by yfiM and yfiN (34). We constructed linearmycin-resistant strains (yfiJ^{A152E}) with single deletions of yfiL, yfiM, and yfiN. The strains with ΔyfiM and ΔyfiN mutations no longer resembled biofilms, whereas, surprisingly, the ΔyfiL-containing colony retained biofilm morphology (Table 1). However, the yfiJ^{A152E} ΔyfiL strain was sensitive to lysis when cultured with *Streptomyces* sp. strain Mg1 (Table 1). These observations indicate that biofilm formation and linearmycin resistance are separable phenotypes, and that resistance requires a functional ABC transporter while biofilm formation does not. Consistent with our previous results, deletion of genes encoding important developmental regulators and structural components of biofilms had no effect on linearmycin resistance (27).

Transposon mutagenesis identifies additional genes required for YfiLMN-mediated biofilm formation. Expression of the yfiLMN operon alone was sufficient to cause *B. subtilis* to form biofilms (Fig. 2 and Table 1). This observation is particularly provocative because *B. subtilis* biofilm formation on minimal salts glutamate glycerol medium (MSgg) occurs concurrently with numerous changes in gene expression (35). Therefore, we asked how YfiLMN causes biofilm formation. Based on protein sequence alignments, YfiLMN belongs to a class of ABC exporters (34). However, based on the ability of the yfiJ^{A152E} ΔyfiL strain to form biofilms (Table 1), active transport likely is not required for formation of biofilm morphology. Therefore, we used transposon mutagenesis to identify genes whose products are necessary for the formation of biofilm morphology but are not transcriptionally regulated by YfiK. We introduced pMarA (36), a transposon mutagenesis plasmid, into the yfiJ^{A152E} strain background. We screened 13,577 yfiJ^{A152E} colonies for mutants that failed to form biofilm morphology. Assuming an average ORF size of 965 bp (4,372 ORFs/4.2 Mbp) (37), we estimate the probability of screen saturation to be 0.96 (38). We identified numerous non-biofilm-forming colony variants. For instance, we commonly identified mucoid variants and verified identified insertions in the eps operon (39). However, we were most interested in 11 transposon insertion mutants (0.08% total) that reverted to wild-type colony morphology. We extracted genomic DNA from the 11 linked transposon insertion mutants and

TABLE 2 Transposon insertion loci identified in loss-of-biofilm-formation screen

Insertion position ^a	Identity ^d	Gene and/or product	Annotated function
76954(−)	IGR _{hprT-ftsH}	<i>hprT</i> , hypoxanthine phosphoribosyltransferase <i>ftsH</i> , ATP-dependent metalloprotease	Purine salvage and interconversion, control of <i>ftsH</i> expression Cell division protein and general stress protein (class III heat shock)
423837(+)	<i>gerKB</i>	Subunit of GerK germination receptor	Spore germination
1525015(+) ^b	IGR _{rpoY-yrkA}	<i>rpoY</i> , RNA polymerase ϵ subunit <i>yrkA</i> , putative membrane-associated protein	Control of RNA polymerase activity Unknown
1866388(−)	IGR _{ymaF-miaA}	<i>ymaF</i> , unknown <i>miaA</i> , tRNA isopentenylpyrophosphate transferase	Unknown tRNA modification
2300897(+) ^c	<i>ilvD</i>	Dihydroxy acid dehydratase	Biosynthesis of branched-chain amino acids
2328299(+)	<i>ypvA</i>	Similar to ATP-dependent helicase	Unknown
2625166(+)	<i>dnaJ</i>	Heat shock protein (activation of DnaK)	Protein quality control
2627755(+)	<i>dnaK</i>	Class I heat shock protein (molecular chaperone)	Protein quality control
2729794(+)	<i>azlB</i>	Lrp family repressor of the <i>azlBCD-brnQ-yrdK</i> operon	Regulation of branched-chain amino acid transport
2887777(+)	IGR _{tig-ysoA}	<i>tig</i> , trigger factor (prolyl isomerase) <i>ysoA</i> , putative hydrolase	Nascent polypeptide folding Unknown
3856278(+)	BSU_MISC_RNA_57	T-box upstream of <i>thrZ</i>	Regulation of <i>thrZ</i> expression

^aInsertion nucleotide number and strand orientation are with respect to a sequenced genome of *B. subtilis* (GenBank accession number [AL009126.3](https://www.ncbi.nlm.nih.gov/nuccore/AL009126.3)).

^bThis insertion was identified in two independent isolates.

^cThis insertion has a phenotype in *yfiJ*^{A152E} but not *yfiJ*⁺ but does not lead to nonbiofilm colony morphology.

^dIGR, intergenic region.

identified the position of each transposon insertion (Table 2). Here, we note that each transposon insertion mutant remained linearmycin resistant, indicating that *yfiJK-LMN* was unaffected during the screen.

The functions identified in the screen do not fall into any known *B. subtilis* colony development pathways. However, we note a pattern for transposon insertions in and near ORFs associated with protein folding and quality control. We identified transposon insertions in *dnaJ*, in *dnaK*, in the intergenic region between *hprT* and *ftsH*, and upstream of *tig* (Table 2). DnaJ and DnaK are components of a molecular chaperone complex involved in class I heat shock response (40, 41). FtsH is a membrane-anchored metalloprotease with diverse functions that include biofilm formation, heat shock response, and chaperone activity (42–44). Tig is a ribosome-associated trigger factor that promotes the proper folding of nascent polypeptides (45). The transposon insertions we identified in *dnaJ* and *dnaK* occur near the 3' and 5' ends, respectively, of the coding sequences and likely disrupt the function of both proteins. It is known that the expression of *ftsH* is regulated by a complex formed by HprT and TilS (46). Therefore, the transposon insertion may have polar effects on *ftsH* expression. Likewise, the transposon insertion upstream of *tig* may influence *tig* expression, which could lead to a change in biofilm formation through loss of chaperone activity.

We also identified branched-chain amino acids as a possible biofilm-related function. First, we identified an insertion in *azlB*, which encodes an Lrp family repressor of the *azlBCD-brnQ-yrdK* operon. This operon contains genes involved in transport of branched-chain amino acids (47). Second, we also identified a transposon insertion in *ilvD*, which encodes a dihydroxy acid dehydratase involved in branched-chain amino acid biosynthesis (48). Disruption of *ilvD* in a *yfiJ*^{A152E} background results in colonies with diminished wrinkles and increased mucoidy but otherwise had no visible phenotype in a *yfiJ*⁺ background (Fig. S4). Branched-chain amino acids are used by *B. subtilis* as precursors for anteiso-branched-chain fatty acid biosynthesis. Supplementation of isoleucine into culture medium causes *B. subtilis* to produce more anteiso-branched-chain fatty acids (17), which influences membrane fluidity and may affect membrane protein dynamics. However, we found that isoleucine supplementation had no effect on either *yfiJ*⁺ or *yfiJ*^{A152E} strains (Fig. S5). Additional characterization is required to determine how *azlB*, *ilvD*, and the other identified transposon insertions influence YfiLMN-mediated biofilm formation.

The YfiJK system responds to linearmycins. We were interested in identifying the signal(s) that naturally activates the YfiJK-LMN system. We first analyzed results from a

large-scale transcriptional analysis of *B. subtilis* grown under 269 different conditions (32). In that study, under all conditions, expression of the *yfiLMN* operon was low and did not appreciably change (Fig. S1B and C). These transcriptional profiling experiments suggest that the YfiJK system is not activated when *B. subtilis* is cultured in isolation.

We reasoned that because YfiJK confers linearmycin resistance, it may respond to linearmycins and become activated during competition with *Streptomyces* sp. strain Mg1. To test this hypothesis, we constructed a *B. subtilis* strain with a transcriptional fusion of the *yfiLMN* promoter to *lacZ* (P_{yfiLMN} -*lacZ*) and cultured the strain with *Streptomyces* sp. strain MG1 on medium containing 5-bromo-4-chloro-3-indolyl- β -D-galactopyranoside (X-Gal). We found that the P_{yfiLMN} -*lacZ* reporter was activated in the portion of the colony immediately adjacent to *Streptomyces* sp. strain Mg1 (Fig. 3A). As a control, we verified that *yfiJ*^{A152E} strains constitutively activated the P_{yfiLMN} -*lacZ* reporter and that the phosphoacceptor histidine (H201) was required for downstream signaling (Table 3) (27). To determine if the YfiJK system responds to linearmycins, we cultured the reporter strain with an Mg1 Δ *lnyI* strain that is unable to produce linearmycins (B. C. Hoefler, R. M. Stubbendieck, N. K. Josyula, S. M. Moisan, E. M. Schulze, and P. D. Straight, unpublished data). We found that P_{yfiLMN} -*lacZ* was not activated by the Mg1 Δ *lnyI* strain (Fig. 3A). As a direct test that the YfiJK system responds to linearmycins, we spotted isolated linearmycins on top of a pregrown *B. subtilis* colony. Over the following day, we observed that the *B. subtilis* colony was lysed from the inside out. We observed strong activation of the reporter on the periphery of the lysed region of the colony (Fig. 3B). Together, these results demonstrate that the YfiJK system responds to linearmycins directly and not to some other product produced by *Streptomyces* sp. strain Mg1.

Expression of the *yfiLMN* operon is induced by multiple polyenes. A characteristic feature of the linearmycins is the presence of multiple conjugated double bonds (29, 30). This polyene moiety is also present in several structurally related molecules that target the cytoplasmic membrane of fungi. Polyene antibiotics interact with ergosterol, which leads to membrane permeabilization and fungal cell death (49–52). Because YfiJ is a membrane-anchored histidine kinase, we hypothesized that linearmycins are sensed directly or as a secondary consequence of perturbation to the *B. subtilis* membrane. Therefore, we asked if other polyenes activate YfiJK signaling or if activation is due to lytic stresses. First, we tested a linear polyene, ECO-02301, that also causes lysis of *B. subtilis* (27, 53). Similar to linearmycin exposure, we observed that ~12 nmol of ECO-02301 lyses *B. subtilis* and activates the P_{yfiLMN} -*lacZ* reporter (Fig. 3B). We next tested the effects of ~16 nmol of the cyclic polyenes amphotericin B and nystatin. While the cyclic polyenes do not lyse *B. subtilis*, weak activation of the P_{yfiLMN} -*lacZ* reporter is visible and demonstrates that activation of YfiJK signaling is not dependent upon lysis (Fig. 3B). As a control, we also tested daptomycin, a structurally unrelated lipopeptide that also lyses *B. subtilis* (27, 54). In contrast to the polyenes, lytic concentrations of daptomycin do not activate the P_{yfiLMN} -*lacZ* reporter (Fig. 3B).

We observed that the strongest activation of the P_{yfiLMN} -*lacZ* reporter was caused by linearmycin exposure (Fig. 3B). Based on high-performance liquid chromatography (HPLC) measurements, we estimate that we spotted between 3 and 5 nmol of linearmycins onto *B. subtilis*, substantially less than the ~12 and ~16 nmol of ECO-02301 and cyclic polyenes used, respectively. This estimation suggests that YfiJK signaling is most strongly activated specifically by linearmycins. Intriguingly, we previously found that a linearmycin-resistant mutant was only weakly cross-resistant to ECO-02301, despite linearmycin and ECO-02301 sharing a similar polyketide backbone (27). Taken together, our results indicate that linearmycins and not lytic membrane stress activate YfiJK signaling and that the YfiJK system is tuned specifically for linearmycins.

Polyene exposure provides subsequent protection against linearmycins. We hypothesized that if expression of the *yfiLMN* operon is induced by polyenes, then *B. subtilis* should become more resistant to subsequent linearmycin exposure. We precultured wild-type *B. subtilis* in increasing concentrations of nystatin and then exposed

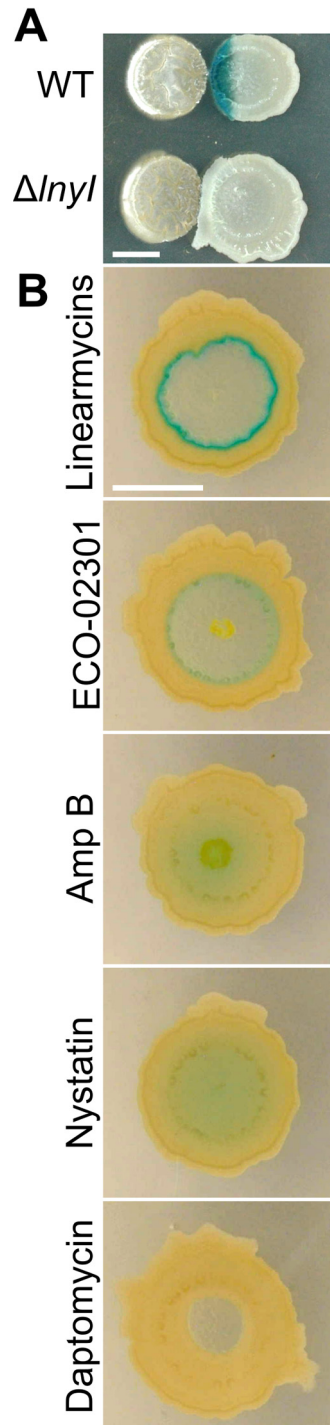


FIG 3 YfjK signaling is activated by linearmycins and other polyenes. (A) A strain of *B. subtilis* (right) with a P_{yFLMN} -*lacZ* reporter (PDS0838) was cultured with either wild-type (WT) *Streptomyces* sp. strain Mg1 (PDS0543) or the *Streptomyces* sp. strain Mg1 $\Delta Inyl$ mutant (PDS0755) (left), which does not produce linearmycins. The photograph was taken after 72 h of coincubation of MYM agar with X-Gal. The photograph is representative of quadruplicate samples. The brightness and contrast were adjusted to better show the blue color. (B) The indicated specialized metabolites were spotted on top of pregrown *B. subtilis* colonies (PDS0838). The photographs were taken from the bottom of the culture dish after *B. subtilis* colonies were exposed to the compounds for 24 h. The appearance of blue indicates activation of P_{yFLMN} -*lacZ*. The brightness and contrast were uniformly adjusted across the panels to better show the blue color on the amphotericin B (Amp B)- and nystatin-treated colonies. The scale bar is 5 mm.

TABLE 3 Linearmycin sensing by *B. subtilis* requires the YfiJ TMD but not YfiLMN

Genotype ^a	Activation of P _{yfiLMN} -lacZ ^b	
	Without strain Mg1	With strain Mg1
<i>yfiJ</i> ⁺	–	+
<i>yfiJ</i> ^{A152E}	+	+
<i>yfiJ</i> ^{H201N}	–	–
<i>yfiJ</i> ^{A152E, H201N}	–	–
<i>yfiJ</i> ⁺ Δ <i>yfiLMN</i>	+	++
<i>yfiJ</i> ^{A152E} Δ <i>yfiLMN</i>	–	+
<i>yfiJ</i> Δ ^{TMD}	–	–
<i>yfiJ</i> Δ ^{TMD, A152E}	–	–

^aWild-type alleles are designated with a superscript plus symbol.

^bThe plus and minus symbols indicate the presence or absence, respectively, of blue color as an indication of P_{yfiLMN}-lacZ reporter activation. The double-plus symbol indicates stronger activation of the P_{yfiLMN}-lacZ reporter.

cells to linearmycins. We found that as the preculture nystatin concentration increased, there was a concurrent decrease in *B. subtilis* sensitivity to lysis by linearmycins (Fig. S7). We verified that the increased linearmycin resistance was due to YfiLMN by repeating the experiment with an isogenic Δ *yfiLMN* strain. Without preculture in nystatin, we observed no differences in lysis between the *yfiJ*⁺ and *yfiJ*⁺ Δ *yfiLMN* strains (Fig. 4A). As expected, when we cultured *yfiJ*⁺ *B. subtilis* in nystatin, we observed increased linearmycin resistance. Unexpectedly, preculture in nystatin also protected the *yfiJ*⁺ Δ *yfiLMN* strain from linearmycins. However, this linearmycin protection was reduced compared to that of the *yfiJ*⁺ strain (Fig. 4B). Although nystatin alone can protect *B. subtilis* from linearmycin, expression of the *yfiLMN* operon by nystatin preculture contributes a greater degree of protection against linearmycin (Fig. 4B).

YfiLMN-mediated biofilm morphology requires KinC. We returned to the observation that expression of the *yfiLMN* operon causes *B. subtilis* to form biofilm morphology. We wanted to test if a polyene would induce YfiLMN-mediated morphological changes in *B. subtilis*. As expected, without nystatin we observed that the *yfiJ*^{A152E} strain forms biofilm morphology, whereas the *yfiJ*⁺ strain does not (Fig. 5). However, when we

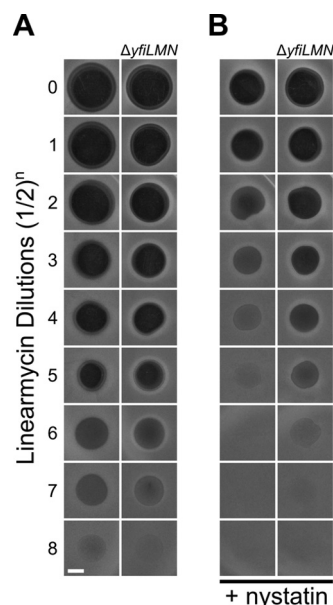


FIG 4 Preconditioning *B. subtilis* in nystatin enhances linearmycin resistance. *yfiJ*⁺ (PDS0571) and *yfiJ*⁺ Δ *yfiLMN* (PDS0798) strains were preconditioned in 0 (A) or 100 (B) μ g/ml nystatin. After embedding *B. subtilis* in agar, 2-fold serial dilutions of linearmycins were plated on top of the agar overlay. Photographs were taken on a black background. Areas of cell lysis appear as dark circles in each panel. The plates were photographed after 18 h of incubation.

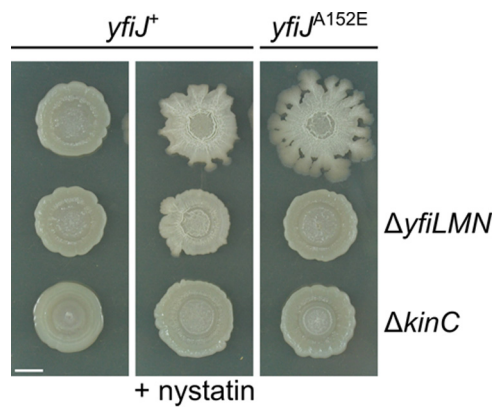


FIG 5 KinC enhances YfiLMN-mediated biofilm formation. *yfiJ*⁺ (PDS0571) and *yfiJ*^{A152E} (PDS0572) strains were cultured on MYM medium containing 0 or 100 $\mu\text{g/ml}$ nystatin. The photographs were taken after 48 h of incubation on MYM agar. The photographs are representative of duplicate samples. The scale bar is 5 mm.

cultured *yfiJ*⁺ with nystatin, we observed biofilm morphology, consistent with previous reports (28). The nystatin-induced *yfiJ*⁺ strain shared similar morphological features with the colony formed by *yfiJ*^{A152E} (Fig. 5). We tested the dependence of nystatin-induced biofilm morphology on YfiLMN by repeating the experiment with $\Delta yfiLMN$ strains. We found that the nystatin-induced *yfiJ*⁺ $\Delta yfiLMN$ strain only weakly formed biofilm morphology, suggesting that nystatin activates expression of the *yfiLMN* operon and causes biofilm colony morphology.

Polyene antibiotics have been shown to activate biofilm formation in *B. subtilis* by triggering K^+ leakage that is sensed by the histidine kinase KinC (28). Therefore, we wanted to determine if the biofilms we observed in nystatin-treated *yfiJ*⁺ strains were due to YfiLMN or KinC. As expected, we found that a *yfiJ*⁺ $\Delta kinC$ strain is mucoid, consistent with defects in biofilm production (28, 44). Intriguingly, the *yfiJ*^{A152E} $\Delta kinC$ strain formed a colony that closely resembled a *yfiJ*⁺ colony (Fig. 5). Similarly, we found that the *yfiJ*⁺ $\Delta kinC$ strain was unable to form a biofilm when induced with nystatin. As both $\Delta kinC$ and $\Delta yfiLMN$ strains were unable to form biofilms under permissive medium conditions or genetic backgrounds, we conclude that both gene products are required for YfiLMN-mediated biofilm morphology. We did not identify *kinC* in the screen of *yfiJ*^{A152E} transposon insertion mutants with loss of biofilm formation. However, because *kinC* mutants form mucoid colonies (28, 44), it is possible that we did not select these colonies when screening for wild-type morphology. Alternatively, we may not have obtained *kinC* transposon insertion mutants because the screen was not fully saturating ($P = 0.96$).

Transposon mutagenesis suggests that YfiJK senses linearmycin-mediated effects. The known mechanisms that microbes use to sense polyenes are indirect. For instance, in the budding yeast *Saccharomyces cerevisiae*, nystatin is sensed by SLN1, which is an osmosensing histidine kinase that senses changes in turgor pressure and detachment of the cytoplasmic membrane from the cell wall (55). Likewise, in *B. subtilis* polyenes are sensed via K^+ leakage by KinC (28). As a first approach to ask if linearmycins are indirectly sensed, we used transposon mutagenesis. Specifically, we asked if we could identify a mutant that constitutively activates YfiJK signaling. We introduced pMarA into a strain with the P_{yfiLMN} -*lacZ* reporter and screened for colonies that constitutively hydrolyzed X-Gal. From a screen of 18,002 colonies, we found 2 blue isolates (0.01% total). However, in both isolates we found that the transposon insertion disrupted *lacR*. LacR is a transcriptional repressor for expression of *lacA*, which encodes an endogenous β -galactosidase. Thus, the blue color in these transductants resulted in constitutive *lacA* expression and not activation of the P_{yfiLMN} -*lacZ* reporter construct (56). We estimate the probability of screen saturation to be 0.98. Although inconclusive, the results and density of this transposon screen suggest that *B.*

subtilis senses linearmycin directly and that transposon insertion mutants cannot reproduce the effects of linearmycin exposure. To further characterize how *B. subtilis* senses linearmycins, we sought to identify the linearmycin sensor.

YfiLMN is not required for *B. subtilis* to respond to linearmycins. We previously reported similarities between the YfiJK-LMN system and peptide sensing and detoxification (PSD) modules encoded in the *B. subtilis* genome (27). For instance, the genetic context for *yfiJK-LMN*, with TCS system and related ABC transporter functions encoded side by side, is identical to the organization of the PSD modules (25, 57). The bacitracin sensing and detoxification system BceABRS is currently the best-characterized PSD system (19, 58–65). The histidine kinase BceS lacks predicted PAS signaling domains, which are often found in histidine kinases (66), or a recognizable extracellular sensor sequence. Instead, the ABC transporter BceAB is responsible for both sensing and detoxifying peptide antibiotics (59, 62).

Similar to BceS, YfiJ has no canonical PAS domains, and protein domain analysis predicted five to six transmembrane helices with no substantial extracellular sensing domain (≤ 17 residues). Given the structural and genetic context similarities between YfiJ and BceS, we wanted to test if YfiLMN is required for *B. subtilis* to respond to linearmycins. We cultured $\Delta yfiLMN$ strains with *Streptomyces* sp. strain Mg1 and found that the P_{yfiLMN} -*lacZ* reporter still responded to *Streptomyces* sp. strain Mg1 (Table 3; Fig. S6). Thus, unlike the bacitracin sensing system, YfiLMN is not required for *B. subtilis* to sense linearmycins. Unexpectedly, in the absence of *Streptomyces* sp. strain Mg1, we observed a reproducible faint blue color in the *yfiJ*⁺ $\Delta yfiLMN$ strain (Fig. S6A). However, during coculture with *Streptomyces* sp. strain Mg1, we observed that the *yfiJ*⁺ $\Delta yfiLMN$ strain more strongly activated the P_{yfiLMN} -*lacZ* reporter. The *yfiJ*^{A152E} $\Delta yfiLMN$ strain behaved similarly to the *yfiJ*⁺ strain and only activated the P_{yfiLMN} -*lacZ* reporter in response to *Streptomyces* sp. strain Mg1 (Fig. S6B; Table 3). Although YfiLMN is not required for *B. subtilis* to sense linearmycins, this observation does not preclude a model where YfiJ and YfiLMN interact, similar to BceS and BceAB (60). We speculate that in the absence of linearmycins, YfiLMN inhibits activation of wild-type *yfiJ*⁺. Linearmycins activate YfiJ and relieve repression by YfiLMN (Fig. S6C). However, the normally constitutively active *yfiJ*^{A152E} requires YfiLMN, which suggests that the A152E charge substitution interferes with an interaction interface between the histidine kinase and the ABC transporter (Fig. S6D).

YfiJ requires the transmembrane domain for *B. subtilis* to respond to linearmycins. Because YfiLMN was dispensable for *B. subtilis* to respond to linearmycins, the most feasible identity of the linearmycin sensor was YfiJ. For some membrane-anchored histidine kinases, the transmembrane domain modulates signaling but is dispensable for signal sensing (67, 68). Therefore, we wanted to determine if the transmembrane domain in YfiJ (YfiJ^{TMD}) is required for linearmycin sensing. We generated a *yfiJ* variant where we replaced the sequence that encodes the transmembrane helices with a new start codon (*yfiJ*^{ΔTMD}). We cultured the *yfiJ*^{ΔTMD} strain with *Streptomyces* sp. strain Mg1 and found that there was no activation of the P_{yfiLMN} -*lacZ* reporter (Table 3). Furthermore, when we cultured the *yfiJ*^{ΔTMD, A152E} strain with *Streptomyces* sp. strain Mg1, we observed no activation of the P_{yfiLMN} -*lacZ* reporter (Table 3). As *yfiJ*^{A152E} strains constitutively express the *yfiLMN* operon even in the absence of linearmycins (27) (Table 3), we hypothesize that membrane anchoring by the TMD is required for proper folding of YfiJ or additional regulatory functions, such as phosphorylation of YfiK.

DISCUSSION

In this study, we used a model system to determine how a *B. subtilis* TCS system senses a chemical challenge from its competitor, *Streptomyces* sp. strain Mg1. In this case, the signaling system encoded by *yfiJK-LMN* elicits appropriate dual responses to bacterial competition, antibiotic resistance, and biofilm formation. The YfiJK-LMN TCS-ABC transporter system responds principally to linearmycins produced by *Streptomyces* sp. strain Mg1, which lyse *B. subtilis* (27, 31). Based on the specificity of activation by

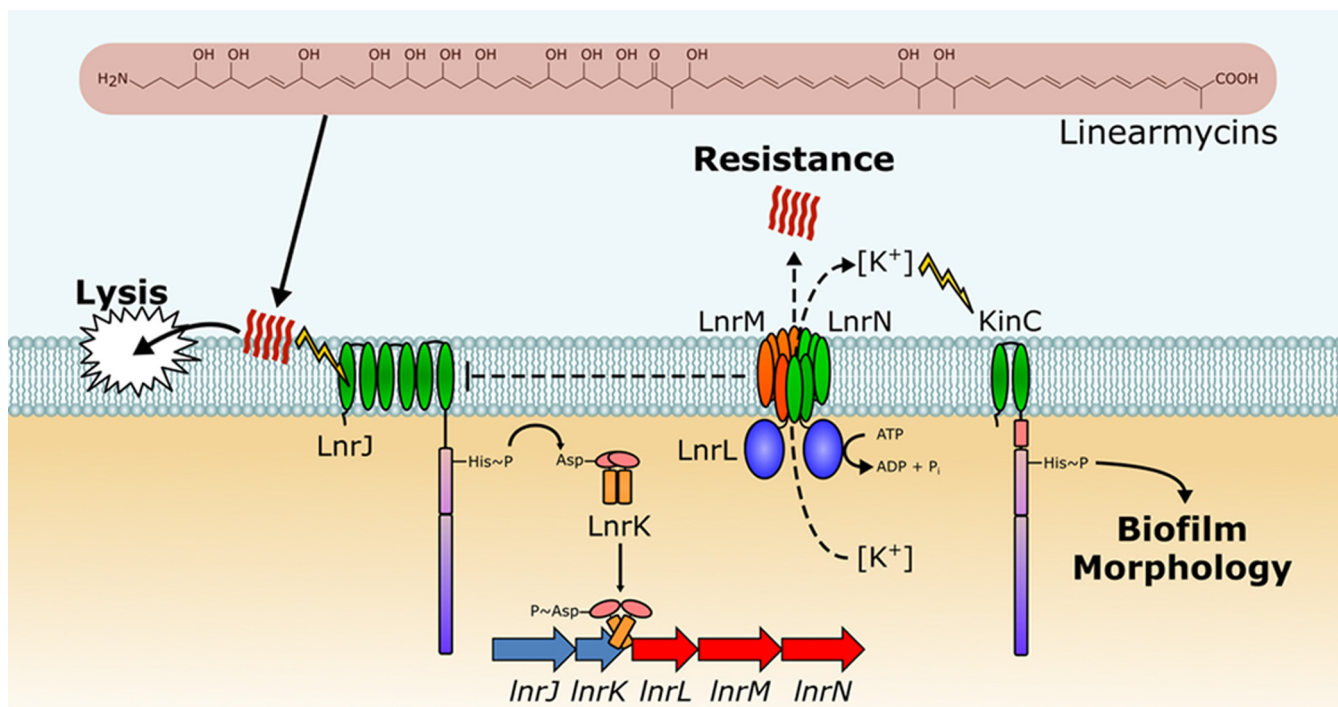


FIG 6 Model for the LnrJK-LMN system. Linearmycins (red squiggles) cause lysis of *B. subtilis*. The linearmycins also activate the histidine kinase LnrJ. Subsequently, the phosphate group is transferred to the cognate response regulator LnrK. Phosphorylated LnrK activates expression of the *lnrLMN* operon, which encodes a linearmycin resistance ABC transporter. LnrLMN presumably removes linearmycins from the membrane (dashed arrow). LnrLMN may regulate LnrJ (dashed arrow). High levels of LnrLMN also indirectly cause KinC enhanced biofilm morphology, possibly due to K⁺ leakage (dashed arrow).

linearmycins, we rename *yfJK-LMN* to *lnrJK-LMN* for linearmycin sensing and response (Fig. 6). Here, we showed that the histidine kinase LnrJ senses linearmycins and other polyenes (Fig. 3A and Table 3) through its transmembrane domain (Table 3). LnrJ phosphorylates its cognate response regulator LnrK, which activates expression of the *lnrLMN* operon (see Fig. S1A and S2 in the supplemental material) (27). Together, *lnrL*, *lnrM*, and *lnrN* encode a linearmycin resistance ABC transporter that also mediates KinC-dependent biofilm morphology (Fig. 2 and 5). Further, we found that *lnrM* and *lnrN*, but not *lnrL*, are required for biofilm formation by linearmycin-resistant *B. subtilis* mutants (Table 1). Using transposon mutagenesis, we identified other genes that are required for LnrLMN-mediated biofilm formation. In particular, our screen highlights functions involved in protein folding and quality control as being involved in biofilm morphology (Table 2).

We were interested in determining how linearmycin-resistant *B. subtilis* colonies form biofilms. Because LnrK only regulates the *lnrLMN* operon (Fig. S1A and S2), we targeted this operon to determine its effects on biofilm morphology. We deleted the *lnrLMN* operon in the *lnrJ^{A152E}* strain and found that the resulting colonies were indistinguishable from the wild type. Further, we found that constitutive expression of the *lnrLMN* operon caused *lnrJ⁺* strains to form biofilms (Fig. 2 and Table 1). We found that that *lnrM* and *lnrN* were required for the *lnrJ^{A152E}* mutant to develop biofilm morphology but *lnrL* was not. However, all three genes, *lnrL*, *lnrM*, and *lnrN*, were required for linearmycin resistance (Table 1). Taken together, these results indicate that the *lnrLMN* operon encodes a multifunctional ABC transporter involved in dual biofilm formation and linearmycin resistance functions. This is in contrast to known ABC transporters that function solely in antibiotic resistance and to conventional *B. subtilis* biofilm development, which requires transcriptional regulation of many genes to affect colony development (34, 35).

We note that the biofilm morphology we investigated shares several features, including dependence upon EPS and *kinC*, with standard *B. subtilis* biofilms cultured on

MSgg (27, 39, 44) (Fig. 5). However, because gene expression profiles are not shared between LnrLMN-mediated biofilms and MSgg biofilms, these structures are not identical. We previously found that deletion of the biofilm matrix regulator DegU abolishes the biofilm phenotype of *InrJ*^{A152E} strains (27, 69). However, we did not identify any transposon insertions in genes associated with matrix functions, although we excluded mutant isolates exhibiting mucoidy, which may be a common characteristic of matrix mutants (Table 2). Currently, we do not know if other components of the MSgg-cultured *B. subtilis* biofilm extracellular matrix contribute to LnrLMN-mediated biofilm morphology.

We found that linearmycin resistance and biofilm morphology are separable phenotypes that depend on the conformation and functionality of LnrLMN. In the cytoplasm, the NBDs of ABC transporters form soluble dimers, which are thought to act as an initiation step in ABC transporter complex assembly (70). Incorporation of the NBDs is necessary for ABC transporter function, which we observe with LnrL, the NBD for LnrLMN. The *InrJ*^{A152E} Δ *InrL* strain formed a biofilm but was sensitive to lysis by *Streptomyces* sp. strain Mg1 (Table 1), confirming that linearmycin resistance requires active ATP hydrolysis. Because the biofilm morphology only requires LnrM and LnrN, we hypothesize either the abundance of the proteins in the membrane or their assembly into hetero-oligomeric complexes causes the observed morphological changes to the colonies. In *Escherichia coli* the maltose ABC transporter MalFGK₂ can form from multiple assembly pathways. All possible intermediate pairwise combinations of MalK (NBD), MalF (MSD), and MalG (MSD) were observed *in vivo* and found to be stable. This includes heterodimeric MalFG MSD dimers (71). Further, MalFG dimers have been purified from *E. coli* and reassembled *in vitro* with MalK₂ to form functional ABC transporter complexes (72). These observations suggest that ABC transporter complexes assemble in the absence of their NBDs (71), potentially having membrane activities distinct from active transport. The *InrJ*^{A152E} mutant expresses the *InrLMN* operon ~135-fold over the wild type (Fig. S2). Perhaps these higher expression levels of *InrM* and *InrN* ultimately result in stable LnrMN heterodimers forming in the membrane. Although LnrMN heterodimers lack LnrL and ATPase activity, the heterodimer may facilitate biofilm formation as a secondary effect of membrane perturbation. Alternatively, formation of excess LnrLMN or LnrMN complexes in the membrane may generate pores that promote K⁺ leakage and trigger biofilm formation (28). In support of the latter model, we found that *kinC* is necessary for LnrLMN-mediated biofilm morphology (Fig. 5 and 6).

As an alternative approach to understanding the biofilm phenotype of LnrLMN, we used transposon mutagenesis and identified *InrJ*^{A152E} mutants that failed to form biofilms. In 4/11 mutants, there were insertions associated with genes encoding chaperone and protein quality control systems. Currently, we do not know how the LnrLMN transporter complex is formed. However, for the MalFGK₂ ABC transporter complex, MalK acts as a chaperone for assembly of MalFG (72, 73). Therefore, it is not unprecedented that MSDs such as LnrM and LnrN may require chaperones to fold. We note that all transposon insertion mutants that we identified were linearmycin resistant, indicating sufficient functional complexes for resistance in the absence of any single chaperone system. We hypothesize that under conditions of elevated LnrLMN production, proper folding and membrane insertion are particularly challenged, increasing the need for chaperones. Perhaps the disruptions in *dnaJ* and *dnaK* affect the folding status of LnrLMN complexes, while insertions near *ftsH* and *tig* affect protein stress response and mitigate membrane stress caused by LnrLMN. Subsequent work is still required to determine if there are functional consequences for *B. subtilis* forming LnrLMN-mediated biofilms. In either case, we hypothesize a connection between accumulation of LnrMN in the membranes and biofilm formation, which could arise through protein-mediated K⁺ ion leakage, for instance. Nystatin-induced biofilms were previously shown to require KinC in a K⁺-dependent manner (28). Consistent with this idea, we found that nystatin, a membrane-targeting polyene, induces biofilm morphology that is dependent upon KinC and LnrLMN (Fig. 5).

Collectively, our results suggest a model where LnrJ senses perturbations in membrane physiology and triggers biofilm morphology and linearmycin resistance through expression of the *LnrLMN* operon. In addition to chaperones, we also identified genes involved in branched-chain amino acid synthesis and transport as requirements for LnrLMN-mediated biofilm morphology, adding another potential link to membrane function (Table 2). Also, we observed that LnrJ requires its transmembrane domain for signal transduction (Table 3). Currently, we do not know if the mechanism of linearmycin-induced lysis of *B. subtilis* involves direct membrane perturbation. The antifungal mechanism of action of polyene antibiotics related to linearmycin is disputed but is known to require interactions with ergosterol and the cell membrane (49–52). Therefore, we favor a model where linearmycins interfere with the *B. subtilis* cytoplasmic membrane and cause cell lysis. Intriguingly, although daptomycin causes similar cell lysis by interfering with fluid membrane microdomains (54), LnrJ is not activated in response to daptomycin (Fig. 3B). Further, we were unable to identify any transposon insertion mutants that spontaneously activated LnrJ signaling. Consequently, we hypothesize that LnrJ acts as a specific sensor for linearmycin, either directly through binding or indirectly through membrane perturbation. Upon activation of LnrJ signaling, we hypothesize that LnrLMN facilitates linearmycin removal from the cytoplasmic membrane using mechanisms similar to those proposed for ABC lipid exporters (74).

This study of bacterial competition highlights a single TCS system that controls linearmycin resistance and biofilm morphology. TCS systems allow cells to sense and respond to their environment and are chief among the survival strategies used by bacteria. However, the functions and signals sensed by roughly half of the TCS systems encoded in bacterial genomes are currently unknown (75). Similarly to the LnrJK system, these unknown TCS systems are potentially important within the context of bacterial competition. As competition drives dynamics in bacterial communities (3), investigating signaling systems activated during bacterial interactions will likely uncover many unknown TCS system functions and the signals that activate them. By incorporating information about TCS systems and responses into models of bacterial communities, we will gain a more thorough understanding of community dynamics and their influence on the environment at large.

MATERIALS AND METHODS

Bacterial strains, media, and primers. The strains of *B. subtilis* used in this study are listed in Table S1 in the supplemental material. For general propagation and manipulation, we inoculated *B. subtilis* and *Escherichia coli* strains in lysogeny broth (LB; 1% tryptone [Bacto], 0.5% yeast extract [BBL], 0.5% sodium chloride [Sigma]) or on LB agar plates (with 1.5% agar [Bacto]). We maintained Mg1 strains as spore suspensions in water at 4°C. We performed all bacterial cocultures and experiments as previously described on MYM [0.4% malt extract (Bacto), 0.4% yeast extract (BBL), 0.4% D-(+)-maltose monohydrate (Sigma), 1.5% agar (Bacto)] (27). We used chloramphenicol (5 µg/ml), kanamycin (5 µg/ml), MLS (1 µg/ml erythromycin, 25 µg/ml lincomycin), and 5-bromo-4-chloro-3-indolyl-β-D-galactopyranoside (X-Gal) (40 µg/ml) as needed. All primers used for cloning are listed in Table S2. We used *E. coli* XL1-Blue or DH5α for plasmid maintenance and manipulation. We prepared *B. subtilis* genetic manipulations in the 168, PY79, or NCIB3610 $\Delta comI$ (76) strain background with one-step transformation. We used phage SPP1 to transduce the genetic manipulations into the NCIB3610 strain background as previously described (77).

RNA extraction and qRT-PCR. We cultured *B. subtilis* to early stationary phase (optical density at 600 nm [OD₆₀₀], 1 to 1.5), serially diluted the cultures 10⁻⁴, and plated 100-µl aliquots onto MYM plates. We incubated the plates for 24 h at 30°C. We then scraped the lawns of *B. subtilis* into RNAprotect bacterial reagent (Qiagen). We lysed 200 µl of fixed cells using lysozyme (15 mg/ml) with proteinase K (5 mg/ml) digestion for 45 min at ambient temperature with vortexing. To extract RNA, we used TRI Reagent (Sigma) and standard procedures. We removed trace DNA from RNA samples using a Turbo DNA-free kit (Applied Biosystems). We performed quantitative reverse transcription-PCR (qRT-PCR) as previously described (27, 78). All qRT-PCR primers are listed in Table S3.

Construction of *yfiLMN*, *yfiL*, *yfiM*, and *yfiN* deletion and complement strains. To generate the *yfiLMN* deletion strain, we used long-flanking homology (LFH) PCR. We used primers 11 and 75 to amplify an upstream sequence of *yfiL*, primers 79 and 155 to amplify a downstream sequence of *yfiN*, and primers 153 and 154 to amplify the MLS resistance cassette from strain BKE08290. We mixed the three PCR products together and used primers 11 and 79 to amplify an LFH PCR product. We transformed the product directly into a $\Delta yfiJ$ strain (PDS0559) to generate PDS0795. We transduced the linked $\Delta yfiJ$ *yfiLMN::mIs* into wild-type *B. subtilis* NCIB3610 (PDS0742) to generate strain PDS0796. We transduced pDR244 into PDS0796 to generate strain PDS0797 with markerless deletions $\Delta yfiJ$ *yfiLMN* as previously

described (79). To complement the $\Delta yfILMN$ deletion, we transduced constitutively expressed $P_{\text{spac}(C)}$ - $yfILMN$ inserted at the $yhdG$ locus from PDS0717 into the $yfILMN$ deletion strains (27).

To generate single deletions of $yfjL$, $yfjM$, and $yfjN$, we used primers 21 and 81 to amplify DNA containing the given deletions marked with the mls resistance cassette from strains BKE08310, BKE08320, and BKE08330, respectively. The PCR products were directly transformed into PDS0559 to generate $\Delta yfjL$ $\Delta yfjL::mls$ (PDS0917), $\Delta yfjJ$ $\Delta yfjM::mls$ (PDS0810), and $\Delta yfjJ$ $\Delta yfjN::mls$ (PDS0811) strains. As described above, we transduced the mls marked deletions into PDS0742 and used pDR244 to generate markerless deletions $\Delta yfjJ$ $\Delta yfjL$ (PDS0789), $\Delta yfjJ$ $\Delta yfjM$ (PDS0814), and $\Delta yfjJ$ $\Delta yfjN$ (PDS0815). To complement the $yfjI$ deletions, we transduced $lacA::yfjJ^+$ (mls) or $lacA::yfjJ^{A152E}$ (mls) from PDS0562 and PDS0563, respectively.

In vivo transposon mutagenesis. We used plasmid pMarA for *in vivo* transposon mutagenesis of *B. subtilis*. The pMarA plasmid contains a Mariner element under the control of the housekeeping sigma factor σ^A and a temperature-sensitive origin of replication (36). For the screening of loss of biofilm morphology, we transduced pMarA into PDS0572. For the screening of spontaneous activation of P_{yfILMN} - $lacZ$, we transduced pMarA into PDS0838. We selected transductants on kanamycin and MLS. We inoculated single colonies overnight in LB at 30°C with kanamycin and MLS. After overnight growth, we diluted the cultures to an OD_{600} of 0.08 and grew the cultures to an OD_{600} of 0.3 to 0.4 at 30°C with kanamycin. Afterwards, we raised the temperature to 42°C to restrict pMarA replication. When the cultures reached an OD_{600} of 1, we mixed 500- μ l culture aliquots with 500 μ l of 50% glycerol and froze the transposon libraries at -80°C .

Screen for loss of biofilm morphology. To screen for $yfjJ^{A152E}$ mutants with loss of biofilm morphology, we thawed aliquots of the frozen transposon library, serially diluted 100 μ l of the library 10^{-5} in LB, and plated 100 to 150 μ l onto MYM plates containing kanamycin. After 2 days of growth, we screened the plates for colonies with wild-type colony morphology. We passaged each isolate onto LB plates with kanamycin and verified their colony morphologies on MYM plates in monoculture. To verify linkage between the colony morphology phenotype and transposon insertion loci, we prepared lysates from each isolate and transduced the $yfjJ^+$ (PDS0571) and $yfjJ^{A152E}$ (PDS0572) strains. We extracted genomic DNA from each $yfjJ^{A152E}$ transductant with confirmed linkage and a colony phenotype in the $yfjJ^{A152E}$ but not the $yfjJ^+$ strain background.

Identification of transposon insertion loci. We identified transposon insertion loci using degenerate primer PCR, inverse PCR, or single-primer PCR. For degenerate primer PCR we used primers oIPCR-2 and Degen3 with the following cycling conditions: 98°C for 5 min, followed by 25 cycles of 98°C for 45 s, 60°C for 45 s (decreasing 0.5°C/cycle), and 72°C for 2 min. We next used 25 cycles of 98°C for 45 s, 50°C for 45 s, and 72°C for 2 min. For inverse PCR, we digested 5 μ g of genomic DNA with AluI (NEB), TaqI (NEB), or Sau3AI (NEB). We ligated the digested DNA using T4 DNA ligase for 16 h at 16°C at a DNA concentration of 5 ng/ μ l. We used the outward-facing primers oIPCR-1 and oIPCR-2 to amplify a linear product from the ligated circular DNA using Phusion polymerase (NEB) with the following cycling conditions: 98°C for 2 min, followed by 30 cycles of 98°C for 10 s, 57°C for 20 s, and 72°C for 15 s. For insertion loci that could not be identified by either degenerate or inverse PCR, we used single-primer PCR. For single-primer PCR we used primer oIPCR-2 under the following conditions to generate single-stranded DNA: 98°C for 2 min, followed by 30 cycles of 98°C for 30 s, 57°C for 10 s, and 72°C for 2 min. Subsequently, we used 20 cycles of 98°C for 30 s, 30°C for 10 s, and 72°C for 2 min, which allows for inward-facing nonspecific primer pairing. Finally, we used 30 cycles of 98°C for 30 s, 57°C for 10 s, and 72°C for 2 min with a final extension of 2 min. We confirmed the presence of PCR products on 1% agarose gels and purified products before sequencing. All sequencing was performed using nested primer oIPCR-3. In all cases we clearly identified the boundary between the insertion element and genomic sequence.

Construction of transcriptional reporter. We used PePPER (80) to predict promoter sequences for $yfjL$, $yfjM$, and $yfjN$. We identified a promoter that overlaps the stop codon and the predicted rho-independent terminator downstream of $yfjK$ (Fig. 1B). Using primers 173 and 174, we amplified a 200-bp DNA sequence containing the putative $yfjILMN$ promoter with EcoRI and HindIII restriction sites. To generate transcriptional fusions to $lacZ$, we digested the PCR product and plasmid pDG1661 ($amyE::\text{RBS}_{\text{spoVG}}\text{-lacZ cat spc bla}$) (81) with EcoRI and HindIII (NEB). We ligated the digested products together using T4 DNA ligase (NEB). We confirmed plasmid construction by restriction digestion. We transformed the P_{yfILMN} - $lacZ$ reporter plasmid into DS7817 to generate PDS0838 in the NCIB3610 strain background. We transduced the P_{yfILMN} - $lacZ$ reporter construct into other strain backgrounds as needed.

Testing specialized metabolites for activation of the P_{yfILMN} - $lacZ$ reporter. We spotted 2 μ l of an early-stationary-phase culture of PDS0838 onto MYM plates with X-Gal and incubated the plates at 30°C. After 18 h of growth, we spotted a 3- μ l solution containing 15 μ g amphotericin B (Sigma), daptomycin (Ontario Chemicals, Inc.), ECO-02301 (Thallion Pharmaceuticals), or nystatin (Sigma) on top of the *B. subtilis* colonies. We isolated linearmycins from *Streptomyces* sp. strain Mg1. Based upon high-performance liquid chromatography (HPLC) measurement, we estimate that we spotted ~ 5 μ g of linearmycins onto *B. subtilis*. After the spots dried, we returned the plates to the 30°C incubator. We observed the colonies the following day.

Screen for constitutive activation of the P_{yfILMN} - $lacZ$ reporter. To screen for mutants with constitutive activation of the P_{yfILMN} - $lacZ$ reporter, we thawed an aliquot of the frozen transposon library, serially diluted 100 μ l of the library 10^{-4} in LB, and plated 150 μ l onto MYM plates containing kanamycin and X-Gal. After 2 days of growth, we screened the plates for colonies with blue color. We passaged each blue isolate on MYM plates with kanamycin and X-Gal and verified the blue color after 2 days of growth. To verify linkage between the constitutive blue color and transposon insertion loci, we prepared lysates

from each isolate and transduced the parental strain with the P_{yflMN} -*lacZ* reporter. We extracted genomic DNA from each transductant with confirmed linkage and identified insertion loci as described above.

SUPPLEMENTAL MATERIAL

Supplemental material for this article may be found at <https://doi.org/10.1128/JB.00186-17>.

SUPPLEMENTAL FILE 1, PDF file, 7.1 MB.

ACKNOWLEDGMENTS

We thank Neha Deshpande, Huajun Han, Donna Iadarola, Yifan Ma, and Paul Merlau for assistance with experiments related to this project. We thank Jennifer Herman for comments and suggestions for the manuscript. Daptomycin was a gift from Jared Silverman (Cubist Pharmaceuticals), and ECO-02301 was a gift of Thallion Pharmaceuticals. Strains of *B. subtilis* were provided by Daniel Ziegler (*Bacillus* Genetic Stock Center) and Wade Winkler (University of Maryland). Instrumentation for qRT-PCR was provided by Craig Kaplan and Dorothy Shippen.

This work, including the efforts of Paul D. Straight, was funded by NSF | NSF Office of the Director (OD) (MCB-1253215).

REFERENCES

- Foster KR, Bell T. 2012. Competition, not cooperation, dominates interactions among culturable microbial species. *Curr Biol* 22:1845–1850. <https://doi.org/10.1016/j.cub.2012.08.005>.
- Stubbendieck RM, Straight PD. 2016. Multifaceted interfaces of bacterial competition. *J Bacteriol* 198:2145–2155. <https://doi.org/10.1128/JB.00275-16>.
- Stubbendieck RM, Vargas-Bautista C, Straight PD. 2016. Bacterial communities: interactions to scale. *Front Microbiol* 7:1–19. <https://doi.org/10.3389/fmicb.2016.01234>.
- Traxler MF, Seyedsayamdost MR, Clardy J, Kolter R. 2012. Interspecies modulation of bacterial development through iron competition and siderophore piracy. *Mol Microbiol* 86:628–644. <https://doi.org/10.1111/mmi.12008>.
- Graff JR, Forschner-Dancause SR, Menden-Deuer S, Long RA, Rowley DC. 2013. *Vibrio cholerae* exploits sub-lethal concentrations of a competitor-produced antibiotic to avoid toxic interactions. *Front Microbiol* 4:8. <https://doi.org/10.3389/fmicb.2013.00008>.
- Wang W, Ji J, Li X, Wang J, Li S, Pan G, Fan K, Yang K. 2014. Angucyclines as signals modulate the behaviors of *Streptomyces coelicolor*. *Proc Natl Acad Sci U S A* 111:5688–5693. <https://doi.org/10.1073/pnas.1324253111>.
- Romero D, Traxler MF, López D, Kolter R. 2011. Antibiotics as signal molecules. *Chem Rev* 111:5492–5505. <https://doi.org/10.1021/cr2000509>.
- Yim G, Wang HH, Davies J. 2007. Antibiotics as signalling molecules. *Philos Trans R Soc Lond B Biol Sci* 362:1195–1200. <https://doi.org/10.1098/rstb.2007.2044>.
- Basler M, Ho BT, Mekalanos JJ. 2013. Tit-for-tat: type VI secretion system counterattack during bacterial cell-cell interactions. *Cell* 152:884–894. <https://doi.org/10.1016/j.cell.2013.01.042>.
- Fabret C, Feher VA, Hoch JA. 1999. Two-component signal transduction in *Bacillus subtilis*: how one organism sees its world. *J Bacteriol* 181:1975–1983.
- Silhavy TJ, Kahne D, Walker S. 2010. The bacterial cell envelope. *Cold Spring Harb Perspect Biol* 2:a000414. <https://doi.org/10.1101/cshperspect.a000414>.
- Rashed R, Veleba M, Kline KA. 2016. Focal targeting of the bacterial envelope by antimicrobial peptides. *Front Cell Dev Biol* 4:55. <https://doi.org/10.3389/fcell.2016.00055>.
- Liu Y, Breukink E. 2016. The membrane steps of bacterial cell wall synthesis as antibiotic targets. *Antibiotics (Basel)* 5:28. <https://doi.org/10.3390/antibiotics5030028>.
- Jordan S, Hutchings MI, Mascher T. 2008. Cell envelope stress response in Gram-positive bacteria. *FEMS Microbiol Rev* 32:107–146. <https://doi.org/10.1111/j.1574-6976.2007.00091.x>.
- Radeck J, Fritz G, Mascher T. 2017. The cell envelope stress response of *Bacillus subtilis*: from static signaling devices to dynamic regulatory network. *Curr Genet* 63:79–90. <https://doi.org/10.1007/s00294-016-0624-0>.
- Beckerling CL, Steil L, Weber MHW, Völker U, Marahiel MA. 2002. Genome-wide transcriptional analysis of the cold shock response in *Bacillus subtilis*. *J Bacteriol* 184:6395–6402. <https://doi.org/10.1128/JB.184.22.6395-6402.2002>.
- Cybulski LE, Albanesi D, Mansilla MCMC, Altabe S, Aguilar PS, de Mendoza D. 2002. Mechanism of membrane fluidity optimization: isothermal control of the *Bacillus subtilis* acyl-lipid desaturase. *Mol Microbiol* 45:1379–1388. <https://doi.org/10.1046/j.1365-2958.2002.03103.x>.
- Mascher T, Margulis NG, Wang T, Ye RW, Helmann JD. 2003. Cell wall stress responses in *Bacillus subtilis*: the regulatory network of the bacitracin stimulon. *Mol Microbiol* 50:1591–1604. <https://doi.org/10.1046/j.1365-2958.2003.03786.x>.
- Ohki R, Giyanto Tateno K, Masuyama W, Moriya S, Kobayashi K, Ogasawara N. 2003. The BceRS two-component regulatory system induces expression of the bacitracin transporter, BceAB, in *Bacillus subtilis*. *Mol Microbiol* 49:1135–1144. <https://doi.org/10.1046/j.1365-2958.2003.03653.x>.
- Mascher T, Zimmer SL, Smith T-AA, Helmann JD. 2004. Antibiotic-inducible promoter regulated by the cell envelope stress-sensing two-component system LiaRS of *Bacillus subtilis*. *Antimicrob Agents Chemother* 48:2888–2896. <https://doi.org/10.1128/AAC.48.8.2888-2896.2004>.
- Serizawa M, Kodama K, Yamamoto H, Kobayashi K, Ogasawara N, Sekiguchi J. 2005. Functional analysis of the YvrGHb two-component system of *Bacillus subtilis*: identification of the regulated genes by DNA microarray and Northern blot analyses. *Biosci Biotechnol Biochem* 69:2155–2169. <https://doi.org/10.1271/bbb.69.2155>.
- Hyryläinen H-L, Pietiäinen M, Lundén T, Ekman A, Gardemeister M, Murtomäki-Repo S, Antelmann H, Hecker M, Valmu L, Sarvas M, Kontinen VP. 2007. The density of negative charge in the cell wall influences two-component signal transduction in *Bacillus subtilis*. *Microbiology* 153:2126–2136. <https://doi.org/10.1099/mic.0.2007/008680-0>.
- Dubrac S, Bisicchia P, Devine KM, Msadek T. 2008. A matter of life and death: cell wall homeostasis and the WalkR (YycGF) essential signal transduction pathway. *Mol Microbiol* 70:1307–1322. <https://doi.org/10.1111/j.1365-2958.2008.06483.x>.
- Fukushima T, Furihata I, Emmins R, Daniel RA, Hoch JA, Szurmant H. 2011. A role for the essential YycG sensor histidine kinase in sensing cell division. *Mol Microbiol* 79:503–522. <https://doi.org/10.1111/j.1365-2958.2010.07464.x>.
- Staroń A, Finkeisen DE, Mascher T. 2011. Peptide antibiotic sensing and detoxification modules of *Bacillus subtilis*. *Antimicrob Agents Chemother* 55:515–525. <https://doi.org/10.1128/AAC.00352-10>.
- Botella E, Devine SK, Hubner S, Salzberg LI, Gale RT, Brown ED, Link H, Sauer U, Codée JD, Noone D, Devine KM. 2014. PhoR autokinase activity is controlled by an intermediate in wall teichoic acid metabolism that is sensed by the intracellular PAS domain during the PhoPR-mediated phosphate limitation response of *Bacillus subtilis*. *Mol Microbiol* 94:1242–1259. <https://doi.org/10.1111/mmi.12833>.

27. Stubbendieck RM, Straight PD. 2015. Escape from lethal bacterial competition through coupled activation of antibiotic resistance and a mobilized subpopulation. *PLoS Genet* 11:e1005722. <https://doi.org/10.1371/journal.pgen.1005722>.
28. López D, Fischbach MA, Chu F, Losick R, Kolter R. 2009. Structurally diverse natural products that cause potassium leakage trigger multicellularity in *Bacillus subtilis*. *Proc Natl Acad Sci U S A* 106:280–285. <https://doi.org/10.1073/pnas.0810940106>.
29. Sakuda S, Guce-Bigol U, Itoh M, Nishimura T, Yamada Y. 1995. Linearmycin A, a novel linear polyene antibiotic. *Tetrahedron Lett* 36:2777–2780. [https://doi.org/10.1016/0040-4039\(95\)00392-P](https://doi.org/10.1016/0040-4039(95)00392-P).
30. Sakuda S, Guce-Bigol U, Itoh M, Nishimura T, Yamada Y. 1996. Novel linear polyene antibiotics: linearmycins. *J Chem Soc Perkin Trans* 1:2315–2319.
31. Barger SR, Hoefler BC, Cubillos-Ruiz A, Russell WK, Russell DH, Straight PD. 2012. Imaging secondary metabolism of *Streptomyces* sp. Mg1 during cellular lysis and colony degradation of competing *Bacillus subtilis*. *Antonie Van Leeuwenhoek* 102:435–445.
32. Nicolas P, Mäder U, Dervyn E, Rochat T, Leduc A, Pigeonneau N, Bidnenko E, Marchadier E, Hoebcke M, Aymerich S, Becher D, Biscicchia P, Botella E, Delumeau O, Doherty G, Denham EL, Fogg MJ, Fromion V, Goelzer A, Hansen A, Härtig E, Harwood CR, Homuth G, Jarmer H, Jules M, Klipp E, Le Chat L, Lecointe F, Lewis P, Liebermeister W, March A, Mars RAT, Nannapaneni P, Noone D, Pohl S, Rinn B, Rügheimer F, Sappa PK, Samson F, Schaffer M, Schwikowski B, Steil L, Stülke J, Wiegert T, Devine KM, Wilkinson AJ, van Dijk JM, Hecker M, Völker U, Bessières P, Noirot P. 2012. Condition-dependent transcriptome reveals high-level regulatory architecture in *Bacillus subtilis*. *Science* 335:1103–1106. <https://doi.org/10.1126/science.1206848>.
33. Davidson AL, Dassa E, Orelle C, Chen J. 2008. Structure, function, and evolution of bacterial ATP-binding cassette systems. *Microbiol Mol Biol Rev* 72:317–364. <https://doi.org/10.1128/MMBR.00031-07>.
34. Quentin Y, Fichant G, Denizot F. 1999. Inventory, assembly and analysis of *Bacillus subtilis* ABC transport systems. *J Mol Biol* 287:467–484. <https://doi.org/10.1006/jmbi.1999.2624>.
35. Vlamakis H, Chai Y, Beauregard P, Losick R, Kolter R. 2013. Sticking together: building a biofilm the *Bacillus subtilis* way. *Nat Rev Microbiol* 11:157–168. <https://doi.org/10.1038/nrmicro2960>.
36. Le Breton Y, Mohapatra NP, Haldenwang WG. 2006. In vivo random mutagenesis of *Bacillus subtilis* by use of TnYLB-1, a mariner-based transposon. *Appl Environ Microbiol* 72:327–333. <https://doi.org/10.1128/AEM.72.1.327-333.2006>.
37. Barbe V, Cruveiller S, Kunst F, Lenoble P, Meurice G, Sekowska A, Vallenet D, Wang T, Moszer I, Médigue C, Danchin A. 2009. From a consortium sequence to a unified sequence: the *Bacillus subtilis* 168 reference genome a decade later. *Microbiology* 155:1758–1775. <https://doi.org/10.1099/mic.0.027839-0>.
38. Zilsel J, Ma PH, Beatty JT. 1992. Derivation of a mathematical expression useful for the construction of complete genomic libraries. *Gene* 120:89–92. [https://doi.org/10.1016/0378-1119\(92\)90013-F](https://doi.org/10.1016/0378-1119(92)90013-F).
39. Branda SS, González-Pastor JE, Ben-Yehuda S, Losick R, Kolter R. 2001. Fruiting body formation by *Bacillus subtilis*. *Proc Natl Acad Sci U S A* 98:11621–11626. <https://doi.org/10.1073/pnas.191384198>.
40. Schröder H, Langer T, Hartl FU, Bukau B. 1993. DnaK, DnaJ and GrpE form a cellular chaperone machinery capable of repairing heat-induced protein damage. *EMBO J* 12:4137–4144.
41. Szabo A, Langer T, Schröder H, Flanagan J, Bukau B, Hartl FU. 1994. The ATP hydrolysis-dependent reaction cycle of the *Escherichia coli* Hsp70 system DnaK, DnaJ, and GrpE. *Proc Natl Acad Sci U S A* 91:10345–10349. <https://doi.org/10.1073/pnas.91.22.10345>.
42. Deuerling E, Mogk A, Richter C, Purucker M, Schumann W. 1997. The ftsH gene of *Bacillus subtilis* is involved in major cellular processes such as sporulation, stress adaptation and secretion. *Mol Microbiol* 23:921–933. <https://doi.org/10.1046/j.1365-2958.1997.2721636.x>.
43. Schumann W. 1999. FtsH—a single-chain charonin? *FEMS Microbiol Rev* 23:1–11.
44. Yepes A, Schneider J, Mielich B, Koch G, Garcia-Betancur J-C, Ramamurthi KS, Vlamakis H, López D. 2012. The biofilm formation defect of a *Bacillus subtilis* flotillin-defective mutant involves the protease FtsH. *Mol Microbiol* 86:457–471. <https://doi.org/10.1111/j.1365-2958.2012.08205.x>.
45. Hoffmann A, Bukau B, Kramer G. 2010. Structure and function of the molecular chaperone trigger factor. *Biochim Biophys Acta* 1803:650–661. <https://doi.org/10.1016/j.bbamcr.2010.01.017>.
46. Lin T-H, Hu Y-N, Shaw G-C. 2014. Two enzymes, TlIS and HprT, can form a complex to function as a transcriptional activator for the cell division protease gene ftsH in *Bacillus subtilis*. *J Biochem* 155:5–16. <https://doi.org/10.1093/jb/mvt081>.
47. Belitsky BR, Gustafsson MC, Sonenshein AL, Von Wachenfeldt C. 1997. An Irp-like gene of *Bacillus subtilis* involved in branched-chain amino acid transport. *J Bacteriol* 179:5448–5457. <https://doi.org/10.1128/jb.179.17.5448-5457.1997>.
48. Mäder U, Hennig S, Hecker M, Homuth G. 2004. Transcriptional organization and posttranscriptional regulation of the *Bacillus subtilis* branched-chain amino acid biosynthesis genes. *J Bacteriol* 186:2240–2252. <https://doi.org/10.1128/JB.186.8.2240-2252.2004>.
49. Odds FC, Brown AJ, Gow NA. 2003. Antifungal agents: mechanisms of action. *Trends Microbiol* 11:272–279. [https://doi.org/10.1016/S0966-842X\(03\)00117-3](https://doi.org/10.1016/S0966-842X(03)00117-3).
50. Baginski M, Sternal K, Czub J, Borowski E. 2005. Molecular modelling of membrane activity of amphotericin B, a polyene macrolide antifungal antibiotic. *Acta Biochim Pol* 52:655–658.
51. Gray KC, Palacios DS, Dailey I, Endo MM, Uno BE, Wilcock BC, Burke MD. 2012. Amphotericin primarily kills yeast by simply binding ergosterol. *Proc Natl Acad Sci U S A* 109:2234–2239. <https://doi.org/10.1073/pnas.1117280109>.
52. Anderson TM, Clay MC, Cioffi AG, Diaz KA, Hisao GS, Tuttle MD, Nieuwkoop AJ, Comellas G, Maryum N, Wang S, Uno BE, Wildeman EL, Gonen T, Rienstra CM, Burke MD. 2014. Amphotericin forms an extramembranous and fungicidal sterol sponge. *Nat Chem Biol* 10:400–406. <https://doi.org/10.1038/nchembio.1496>.
53. McAlpine JB, Bachmann BO, Piraeem M, Tremblay S, Alarco A-M, Zazopoulos E, Farnet CM. 2005. Microbial genomics as a guide to drug discovery and structural elucidation: ECO-02301, a novel antifungal agent, as an example. *J Nat Prod* 68:493–496. <https://doi.org/10.1021/np0401664>.
54. Mueller A, Wenzel M, Strahl H, Grein F, Saaki T, Kohl B, Siersma T, Bandow J, Sahl H, Schneider T, Hamoen L. 2016. Daptomycin inhibits bacterial cell envelope synthesis by interfering with fluid membrane microdomains. *Proc Natl Acad Sci U S A* 113:E7077–E7086. <https://doi.org/10.1073/pnas.1611173113>.
55. Reiser V, Raitt DC, Saito H. 2003. Yeast osmosensor Sln1 and plant cytokinin receptor Cre1 respond to changes in turgor pressure. *J Cell Biol* 161:1035–1040. <https://doi.org/10.1083/jcb.200301099>.
56. Errington J, Vogt CH. 1990. Isolation and characterization of mutations in the gene encoding an endogenous *Bacillus subtilis* beta-galactosidase and its regulator. *J Bacteriol* 172:488–490. <https://doi.org/10.1128/jb.172.1.488-490.1990>.
57. Yamamoto H, Uchiyama S, Sekiguchi J. 1996. The *Bacillus subtilis* chromosome region near 78° contains the genes encoding a new two-component system, three ABC transporters and a lipase. *Gene* 181:147–151. [https://doi.org/10.1016/S0378-1119\(96\)00495-7](https://doi.org/10.1016/S0378-1119(96)00495-7).
58. Bernard R, Joseph P, Guiseppi A, Chippaux M, Denizot F. 2003. YtsCD and YwoA, two independent systems that confer bacitracin resistance to *Bacillus subtilis*. *FEMS Microbiol Lett* 228:93–97. [https://doi.org/10.1016/S0378-1097\(03\)00738-9](https://doi.org/10.1016/S0378-1097(03)00738-9).
59. Bernard R, Guiseppi A, Chippaux M, Foglino M, Denizot F. 2007. Resistance to bacitracin in *Bacillus subtilis*: unexpected requirement of the BceAB ABC transporter in the control of expression of its own structural genes. *J Bacteriol* 189:8636–8642. <https://doi.org/10.1128/JB.01132-07>.
60. Rietkötter E, Hoyer D, Mascher T. 2008. Bacitracin sensing in *Bacillus subtilis*. *Mol Microbiol* 68:768–785. <https://doi.org/10.1111/j.1365-2958.2008.06194.x>.
61. Kingston AW, Zhao H, Cook GM, Helmann JD. 2014. Accumulation of heptaprenyl diphosphate sensitizes *Bacillus subtilis* to bacitracin: implications for the mechanism of resistance mediated by the BceAB transporter. *Mol Microbiol* 93:37–49. <https://doi.org/10.1111/mmi.12637>.
62. Dintner S, Heermann R, Fang C, Jung K, Gebhard S. 2014. A sensory complex consisting of an ATP-binding cassette transporter and a two-component regulatory system controls bacitracin resistance in *Bacillus subtilis*. *J Biol Chem* 289:27899–27910. <https://doi.org/10.1074/jbc.M114.596221>.
63. Fritz G, Dintner S, Treichel S, Radeck J, Gerland U, Mascher T. 2015. A new way of sensing: need-based activation of antibiotic resistance by a flux-sensing mechanism. *mBio* 6:e00975-15. <https://doi.org/10.1128/mBio.00975-15>.
64. Radeck J, Gebhard S, Orchard PS, Kirchner M, Bauer S, Mascher T, Fritz G. 2016. Anatomy of the bacitracin resistance network in *Bacillus subtilis*. *Mol Microbiol* 100:607–620. <https://doi.org/10.1111/mmi.13336>.
65. Fang C, Nagy-Staroń A, Grafe M, Heermann R, Jung K, Gebhard S,

- Mascher T. 2016. Insulation and wiring specificity of BceR-like response regulators and their target promoters in *Bacillus subtilis*. *Mol Microbiol* 104:16–31. <https://doi.org/10.1111/mmi.13597>.
66. Galperin MY, Nikolskaya AN, Koonin EV. 2001. Novel domains of the prokaryotic two-component signal transduction systems. *FEMS Microbiol Lett* 203:11–21. <https://doi.org/10.1111/j.1574-6968.2001.tb10814.x>.
67. Wang LC, Morgan LK, Godakumbura P, Kenney LJ, Anand GS. 2012. The inner membrane histidine kinase EnvZ senses osmolality via helix-coil transitions in the cytoplasm. *EMBO J* 31:2648–2659. <https://doi.org/10.1038/emboj.2012.99>.
68. Foo YH, Gao Y, Zhang H, Kenney LJ. 2015. Cytoplasmic sensing by the inner membrane histidine kinase EnvZ. *Prog Biophys Mol Biol* 118: 119–129. <https://doi.org/10.1016/j.pbiomolbio.2015.04.005>.
69. Verhamme DT, Murray EJ, Stanley-Wall NR. 2009. DegU and Spo0A jointly control transcription of two loci required for complex colony development by *Bacillus subtilis*. *J Bacteriol* 91:100–108. <https://doi.org/10.1128/JB.01236-08>.
70. Kennedy KA, Traxler B. 1999. MalK forms a dimer independent of its assembly into the MalFGK2 ATP-binding cassette transporter of *Escherichia coli*. *J Biol Chem* 274:6259–6264. <https://doi.org/10.1074/jbc.274.10.6259>.
71. Kennedy KA, Gachelet EG, Traxler B. 2004. Evidence for multiple pathways in the assembly of the *Escherichia coli* maltose transport complex. *J Biol Chem* 279:33290–33297. <https://doi.org/10.1074/jbc.M403796200>.
72. Sharma S, Davis JA, Ayvaz T, Traxler B, Davidson AL. 2005. Functional reassembly of the *Escherichia coli* maltose transporter following purification of a MalF-MalG subassembly. *J Bacteriol* 187:2908–2911. <https://doi.org/10.1128/JB.187.8.2908-2911.2005>.
73. Traxler B, Beckwith J. 1992. Assembly of a hetero-oligomeric membrane protein complex. *Proc Natl Acad Sci U S A* 89:10852–10856. <https://doi.org/10.1073/pnas.89.22.10852>.
74. van Meer G, Halter D, Sprong H, Somerharju P, Egmond MR. 2006. ABC lipid transporters: extruders, flippases, or flopless activators? *FEBS Lett* 580:1171–1177. <https://doi.org/10.1016/j.febslet.2005.12.019>.
75. Bekker M, Teixeira de Mattos MJ, Hellingwerf KJ. 2006. The role of two-component regulation systems in the physiology of the bacterial cell. *Sci Prog* 89:213–242. <https://doi.org/10.3184/003685006783238308>.
76. Konkol MA, Blair KM, Kearns DB. 2013. Plasmid-encoded ComI inhibits competence in the ancestral 3610 strain of *Bacillus subtilis*. *J Bacteriol* 195:4085–4093. <https://doi.org/10.1128/JB.00696-13>.
77. Phillips AM, Calvo RA, Kearns DB. 2015. Functional activation of the flagellar type III secretion export apparatus. *PLoS Genet* 11:e1005443. <https://doi.org/10.1371/journal.pgen.1005443>.
78. Vargas-Bautista C, Rahlwes K, Straight P. 2014. Bacterial competition reveals differential regulation of the pks genes by *Bacillus subtilis*. *J Bacteriol* 196:717–728. <https://doi.org/10.1128/JB.01022-13>.
79. Koo B-M, Kritikos G, Farelli JD, Todor H, Tong K, Kimsey H, Wapinski I, Galardini M, Cabal A, Peters JM, Hachmann A-B, Rudner DZ, Allen KN, Typas A, Gross CA. 2017. Construction and analysis of two genome-scale deletion libraries for *Bacillus subtilis*. *Cell Syst* 4:291–305. <https://doi.org/10.1016/j.cels.2016.12.013>.
80. de Jong A, Pietersma H, Cordes M, Kuipers OP, Kok J. 2012. PePPER: a webserver for prediction of prokaryote promoter elements and regulons. *BMC Genomics* 13:299. <https://doi.org/10.1186/1471-2164-13-299>.
81. Guérout-Fleury AM, Frandsen N, Stragier P. 1996. Plasmids for ectopic integration in *Bacillus subtilis*. *Gene* 180:57–61. [https://doi.org/10.1016/S0378-1119\(96\)00404-0](https://doi.org/10.1016/S0378-1119(96)00404-0).